Adjusting the electrostatic and the magnetic boundary conditions of the PROTO-SPHERA experiment: present status and prospects

Franco Alladio[1†], Paolo Micozzi[1], Alessandro Mancuso[1 retired], Vincenzo Zanza[1 retired], Fabrizio Andreoli[1], Gerarda Apruzzese[1], Luca Boncagni[1], Paolo Buratti[1], Michele Caponero[1], Fabio Crescenzi[1], Yacopo Damizia[3], Ocleto D'Arcangelo[1], Francesco Filippi[1], Giuseppe Galatola Teka[5], Francesco Giammanco[4 retired], Edmondo Giovannozzi[1], Danilo Giulietti[5], Luigi Andrea Grosso[1], Matteo Iafrati[1], Alessandro Lampasi[1], Violeta Lazic[1], Davide Liuzza[1], Giuseppe Maffia[2], Simone Magagnino[1], Simone Mannori[1], Paolo Marsili[4], Valerio Piergotti[1], Mario Pillon[1], Selanna Roccella[1], Giuliano Rocchi[1], Alessandro Sibio[1], Benedetto Tilia[1], Brunello Tirozzi[2,3], Angelo Tuccillo[1 retired], Onofrio Tudisco[1] and Ciro Visone[6]

[1]FSN Department, Centro Ricerche ENEA di Frascati, 45, Via E. Fermi, I-00044 Frascati, Italy

[2]CREATE Consortium

[3]Physics Department Università Roma-1, la Sapienza

[4]Università di Pisa

[5]Università di Padova e Consorzio RFX and FSN Department, CR-ENEA Frascati

[6]Università di Napoli Federico-II

(Received xx; revised xx; accepted xx)

[†] Email address for correspondence: franco.alladio@enea.it

In Astrophysics the boundary conditions for plasma phenomena are provided by Nature and the astronomer faces the problem of understanding them from a variety of observations (Hester 1996), on the other hand in laboratory plasma experiments the electromagnetic boundary conditions become a major problem in the set-up of the machine that produces the plasma, an issue that has to be investigated step by step and to be modified and adapted with great patience, in particular in the case of an innovative plasma confinement experiment. The PROTO-SPHERA machine is a magnetic confinement experiment for studying controlled fusion, which emulates in the laboratory the jet + torus plasma configurations often observed in Astrophysics: an inner magnetized jet of plasma centered on the (approximate) axis of symmetry and surrounded by a magnetized plasma torus orthogonal to this jet (Hester 1995). The first and unavoidable difference between PROTO-SPHERA and its cosmical examples is that in Astrophysics the containment force fulfilling the virial theorem is obviously the gravitational one, in the case of a laboratory experiment the virial theorem must be fulfilled by means of the magnetic field produced by poloidal field coils (PF coils), external to the plasma configuration (Shafranov 1966), which are responsible for containing the expansive force of the current carrying plasma torus. The second difference is that the boundaries of some of these astrophysical configurations are often not in static equilibrium but keep on expanding, while slowing down, like in the case of the Supernova remnants (Chevalier 1982). The third difference, which is less obvious, is that in Astrophysics, in the nonrelativistic approximation, the solenoidal condition for the plasma current density $\vec{\nabla} \bullet \vec{j} = 0$ is automatically satisfied everywhere (Spruit 2013); instead in a laboratory experiment there are nearby metallic conductors that the plasma can charge and therefore divergences of the plasma current density can occur; the charging of these metal surfaces can trigger the release of secondary spurious plasma currents.

As in PROTO-SPHERA the plasma is simply connected, i.e. no metal current conducting rod is linked to the plasma torus, while instead it is the inner magnetized plasma jet (in the following called the centerpost) that is linked to the torus, it is required that no spurious plasma current path modifies the optimal shape of the plasma centerpost. Moreover, as the plasma torus is produced and sustained by the inner plasma centerpost through magnetic reconnections (Taylor 1989), it is required as well that spurious current paths do not surround the torus on its outboard, in order not to lower the efficiency of the magnetic reconnections that maintain the plasma torus at the expense of the plasma centerpost. Boundary conditions, through continuous corrections, have fulfilled these two requirements, allowing for the sustainment in steady state (1 sec) of the jet + torus combined plasma configuration inside an insulating transparent cylindrical vacuum vessel, without any need of stabilization by a massive shell-like metal conductor surrounding the plasma.

Key words: astrophysical plasmas, laboratory plasmas, magnetic confinement

---

1. Purpose and aims of the experiment

1.1. Magnetic reconnections in Laboratory and Astrophysical plasmas

The phenomena of magnetic reconnection in astrophysical plasmas are present from the terrestrial Magnetosphere (Southwood et al. 1988), to the solar Corona (Fehlau et al. 1971), until to the Supernovae remnants (Tavani et al. 2011), in order of increasing cosmic scale. These phenomena can be so summarized: near a point, or a curve, where two magnetic field lines touch each other but have opposite field direction (so-called X-points), a "tearing" of those lines occurs, followed by a subsequent different "stitching" between them (Stenzel et al. 1981); the new magnetic field configuration contains a lower energy and so the magnetic reconnections lead to an expulsion of energy from the magnetic field and to the consequent heating of the plasma itself (Stenzel et al. 1982). In the reconnections, in addition to the transfer of energy, there is also a transfer of magnetic flux and of electric current (Fear et al. 2017). The PROTO-SPHERA experiment (Alladio et al. 2001, Alladio et al. 2006) was built at the CR-ENEA in Frascati in order to study an innovative configuration of plasma magnetic confinement, in view of Controlled Fusion research, quite different from the confinement experiments studied up to now.

PROTO-SPHERA is an attempt to emulate in the laboratory the jet + torus plasma of the Crab Nebula (Hester et al. 1995): an internal magnetized centerpost of plasma (jet) on the axis of symmetry of the configuration, surrounded by a magnetized plasma torus orthogonal to the plasma centerpost. The confined plasma geometry is simply connected, as well as the geometry of the machine that encloses it: the vacuum chamber is a cylinder and no metal conductor is topologically linked to the plasma torus. The plasma centerpost is sustained by a DC voltage, applied between electrodes internal to the vacuum vessel, and the plasma torus is formed around the plasma centerpost by magnetic reconnections: the lines of force that wind around the centerpost are broken and reconnected into lines of force that wind around the torus (DC Helicity Injection); therefore the experiment, for all the time in which the centerpost is kept running, is capable of sustaining the torus, provided that the magnetic flux transfer from the former to the latter is large enough.

1.2. *PROTO-SPHERA as a variant of the Tokamak configuration*

The PROTO-SPHERA experiment is a magnetic confinement configuration with rotation symmetry, just like the Tokamak (Wesson 2011): the plasma, studied in view of controlled fusion nuclear reactions, must take the form of a torus and there are two indispensable requirements for confining it. First there must be a toroidal magnetic field B_T (directed along the large circle of the torus) and second a poloidal magnetic field B_{pol} (directed along the small circle of the torus), this last requirement is equivalent to the presence of a toroidal electric current flowing inside the plasma torus. The plasma thus becomes organized according to magnetic flux surfaces, each contained inside another; on every flux surface the lines of magnetic force are wrapped along helices, as in figure 1(*a*).

PROTO-SPHERA tries to overcome some of the limitations of the Tokamaks: it removes the two metal central conductors, hitherto considered fundamental; not only the vertical central conductor (which closes the electric current of the external toroidal magnet, figure 1(*a*), and generates the toroidal magnetic field) but also the finite length straight solenoid transformer coil, whose variable electric current wraps in a Tokamak around the vertical central conductor, figure 1(*a*), and induces the toroidal current in the plasma. Both metal conductors are replaced by a single different conducting material: a current carrying centerpost plasma discharge (CP), with lines of magnetic force and lines of electric current also helically wrapped, see figure 1(*a*). It can be said that PROTO-SPHERA is: "a variant of the Tokamak configuration, in which a central plasma discharge plays the roles of both the central metal conductors and consequently eliminates them".

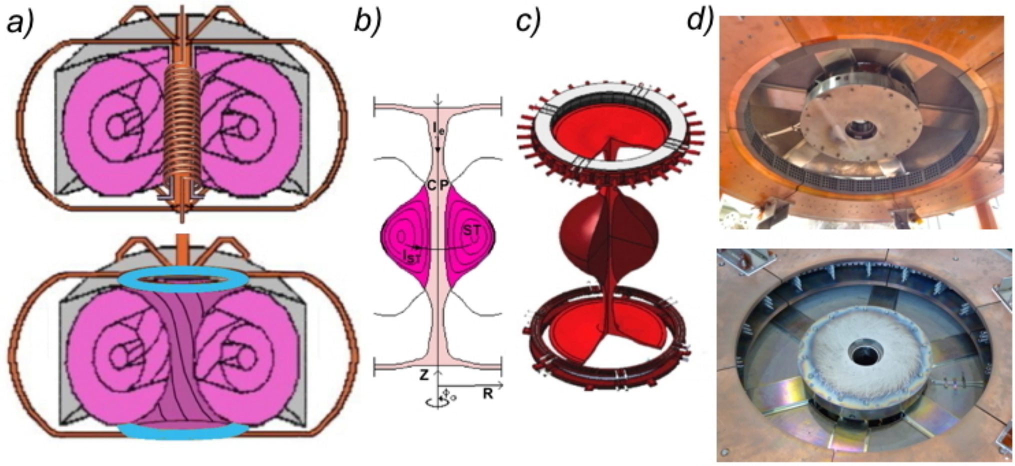

FIGURE 1. (*a*) Scheme of a Tokamak (top) and of PROTO-SPHERA (bottom): pink colour is for plasma, gray for vessel, orange for metal bars, blue for electrodes. (*b*) Poloidal cross-section of PROTO-SPHERA. (*c*) Perspective sketch of the plasma and of the annular electrodes. (*d*) View of the annular anode (top) and of the annular cathode (bottom).

This choice implies an enormous simplification, i.e. the cylindrical shape of the container: the toroidal vacuum chambers are big complications for Tokamaks, already in their construction phase, but even more in the cases where interventions and repairs are necessary. On the other hand the PROTO-SPHERA configuration requires two electrodes (Alladio *et al.* 2000) to be present inside the cylindrical vacuum vessel, shown in figure 1(*b*). The annular form of the electrodes was chosen not only in order to dilute the density of power and of electric current impinging upon them, but also because the "mushroom" shaped plasma in front of both electrodes, shown in figure 1(*c*), stabilizes the overall configuration in ideal MHD (Micozzi et al. 2010). The anode was built as a hollow gas-puffed annular anode, composed of 30 Copper modules, protected on its plasma facing side by tiles of Copper-Tungsten alloy, the gray elements of figure 1(*d*), with 20 holes each in front of the plasma, each module is fed by gas on its rear and the plasma is able to diffuse into the front holes. The cathode is a hot annular cathode, divided in 6 sectors, with a total of 54 Tungsten filaments, shown in figure 1(*d*), heated to about 2900 ºC; the six-phased AC heating of the filaments is switched off just before a DC voltage is applied between the electrodes in order to obtain the plasma break-down. In order to accommodate the electrodes, two AISI304 ferrules, 25 cm tall, were added on top and bottom of the former START Aluminium cylindrical vacuum vessel (2m internal diameter, 4 cm thick, a gift of Culham UKAEA Research Center in 2004), which was used as the first vessel for PROTO-SPHERA: the cylindrical vacuum chamber was then elongated to a total eighth of 2.5 m.

1.3. *A confinement experiment based upon magnetic reconnections*

The presence of a toroidal field BT in PROTO-SPHERA was just the consequence of Maxwell's equations (Ampere's theorem), provided that the electrodes were going to be able to produce the plasma current in the centerpost discharge according to the design specifications. On the other hand that, through a mainly vertical current I_e, produced by the electrodes, it could be possible to sustain a toroidal current I_{ST} flowing in a horizontal direction inside the plasma torus (Taylor 1989), like in figure 1(*b*), was, at the moment of the design, a possibility already explored in other DC Helicity Injection experiments (Nagata *et al.* 1993), but the efficiency of the magnetic flux transfer (expressed by the ratio I_{ST}/I_e between the two orthogonal plasma currents) was unpredictable in this new configuration and therefore became one of the essential aims of the experiment, also for its significance for astrophysical phenomena. This possibility is not a simple consequence of Maxwell's equations and therefore relies on the plasma physics phenomena which allow for the breaking of the magnetic field lines from the centerpost discharge (CP) and permit their reconnection inside the plasma torus (ST), through the magnetic separatrix shown in figure 1(*b*), endowed with two (upper and lower) circles of ordinary X-points (B_{pol}=0, B_T≠0). The most obvious fluid-dynamical analogy is with the smoke rings, that are produced by straight jets of steam from erupting volcanoes (Velasco Fuentes 2014) as well as by skilled cigarettes smokers, but also with the air rings that are produced and supported underwater by playful cetaceans (Paulos 2010). In the magnetic reconnections, in addition to the transfer of energy, there is also a transfer of magnetic flux and of electric current: part of the toroidal electric current, which is wrapped inside the plasma centerpost discharge, is therefore transferred to wrap inside the surrounding torus, right through the tears that occur on the two circles of ordinary X-points.

Many aspects of magnetic reconnection are still today poorly understood (Zweibel 2016): even the reconnection time is assessed differently on the basis of different theoretical models (Loueiro 2016). One of the most interesting aspects of magnetic reconnection is its ability to accelerate, out of thermal equilibrium, the plasma electrons, a characteristic that causes sudden X-ray emissions (Bühler 2014). Furthermore, the magnetic reconnections, by converting a part of the magnetic energy of the field into the kinetic energy of the plasma, are also able to heat the plasma itself (Stenzel 1982), at the level of the thermal part of its distribution function; this characteristic makes magnetic reconnections extremely interesting in the pursuit of Controlled Fusion. A heating method based on internal natural phenomena, produced by the self-organization of the plasma configuration, could prove to be more effective than the heating methods that have to resort to additional heating devices, located outside the machine that produces and confines the plasma, as building the former is often even more complicated than building the latter. The possibility of obtaining the heating of the plasma by magnetic reconnections is suggested by the Astrophysics of the Sun: today a credited hypothesis for the high temperature of the Solar Corona (from 4500-6000 ºK of the underlying Solar Photosphere to millions of ºK of the outer Corona) is that it is due to the magnetized flux tubes rising from the thin solar Tachocline, crossing the whole convective region of the Sun, piercing the Photosphere and the Chromosphere and finally undergoing magnetic reconnections (such as solar flares) and releasing thermal energy to the lower density plasma of the Solar Corona (Parker 1990, Zweibel 2009).

2. Correcting the boundary conditions of the experiment

This paper deals with the first four and a half years of commissioning of PROTO-SPHERA and in particular with the corrections applied to the boundary conditions of the experiment. The main prescription found up to now can be summarized as "try to substitute all metallic parts near the plasma with insulating materials". Only metallic components that could not be dispensed with have remained unaltered near the plasma: electrodes, metal casings of poloidal field coils internal to the vessel and divertor plates facing the plasma tori. These metallic surfaces are relevant as well, not only from the point of view of the plasma-electrode and of the plasma-divertor plate interactions but also because they are charged by the plasma and influence the azimuthal (toroidal) rotation of the plasma; however the boundary conditions connected with the metallic surfaces near the plasma will not be treated in this paper, which will deal only with the non metallic boundary conditions.

As PROTO-SPHERA is a concept assessment experiment, aiming at verifying the feasibility of its innovative confinement scheme, it was consequently built with the constraint of minimizing its costs. As the two main aims of the experiment are to assess the stability of the configuration and the steady-state efficiency of the DC Helicity Injection, it was required that the plasma duration should largely exceed the two corresponding plasma time scales: the Alfvén ideal MHD time ($\tau_A \sim 0.5$ μs) and the resistive diffusion time ($\tau_R \sim 10$ to 250 ms for electron volume average temperatures from 40 to 350 eV). Therefore, in order to simplify all the issues of heat removal from the components internal to the vessel, the plasma sustainment was limited, since its original design, to a maximal duration of 1.1 sec.

Also the additional insulating materials that were introduced during the commissioning were the least expensive ones, i.e. a variety of plastic materials, chosen on the base of their specific properties. If one takes into account the requirements of a future steady state fusion reactor, then one has to consider other insulating materials, such as Aluminium oxynitride (AlON), which is more resilient to thermal and to mechanical stresses than most metals (Corbin 1989) and is also capable to withstand high neutron fluxes (Parker 1985). This composite material is already being industrially produced nowadays, although its recent introduction on the market makes it at moment very expensive.

2.1. *Outline of the progress of the experiment*

PROTO-SPHERA was built and operated in its initial Phase-1 from mid-2014 until the beginning of 2018. Inside the vacuum chamber there were eight poloidal magnetic field coils: the PFInt-B shaping group coils, shown in figure 2(*a*), industrially built, all fed in series and armored by 5 to 10 mm thick AISI304 casings. They are capable of shaping the centerpost plasma, shown also in figure 2(*a*), while almost dividing the plasma discharge in three sections: on top the anodic plasma, in the middle the main equatorial plasma (whose outboard envelopes a sphere with 0.70 m diameter, located within a 0.87 m vertical space between the two PF2 poloidal field mirror coils) and on the bottom the cathodic plasma. The centerpost discharge passes through the holes inside both of the two PF2 coils, which are internally protected by additional Copper-Tungsten cylindrical shells. The poloidal magnetic field reaches in the holes of the PF2 mirror coils its maximal value: about 0.5 T.

In the final Phase-2 of the experiment a new set of six internal armored coils (PFInt-A compression coils) will contain the expansion force of the current carrying spherical tori. The full current of the centerpost plasma, that was the aim of Phase-1: I_e= 10 kA in Hydrogen, was sustained for the duration of 1 sec at the beginning of 2018, see figure 2(*b*). The excellent surprise was that the plasmas produced were as dense as those of high-field Tokamaks (> 10^{20} particles/m^3) and that the central plasma discharges rotated at about 500 turns/sec around their symmetry axes. The azimuthal rotation (Lehnert 1971) is in almost all circumstances a very stabilizing feature (Haverkort 2012) for laboratory plasmas; in astrophysical plasmas it also influences the angular momentum losses and the accretion rates through the magneto-rotational instability (MRI, Velikhov 1959).

In the same year 2018, PROTO-SPHERA produced and sustained as well, for 0.5 seconds, its first plasma tori, carrying a toroidal current up to I_{ST}= 7 kA.

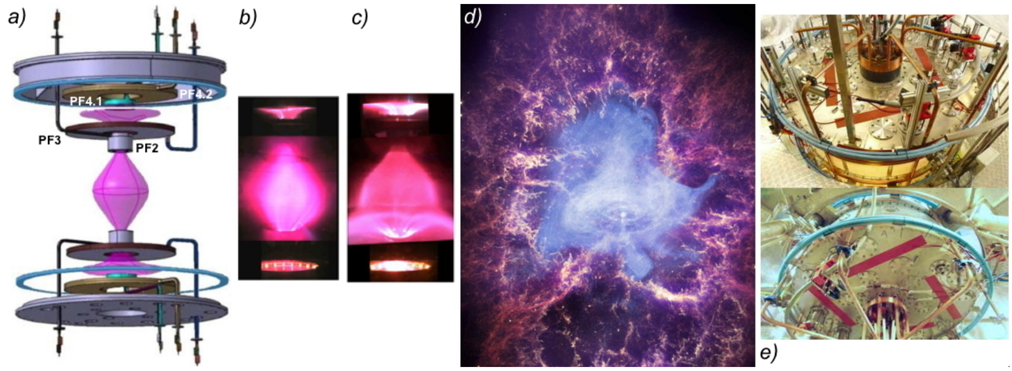

FIGURE 2. (*a*) Scheme of plasma centerpost (pink) and of PFInt-B internal armored coils, the main plasma is limited by the two PF2 mirror coils; the mechanical structures of both electrodes are removed from the scheme. (*b*) Image of Hydrogen plasma centerpost at I_e= 10 kA, shot #969. (*c*) Image of centerpost at I_e= 10 kA & of torus at I_{ST}= 7kA, Hydrogen shot #1280. (*d*) Composite image of Crab nebula from Chandra (X rays), Hubble (visible) and Spitzer (infrared) space telescopes. (*e*) The 4 PExt coils (green-blue) wound around the vacuum vessel.

The tori were indeed quite "lean", as figure 2(*c*) shows, but they were the first emulation of the Crab Nebula configuration (Hester 1996), shown in figure 2(*d*). The tori were obtained by adding four impromptu (PFExt) poloidal magnetic vertical field coils, shown in figure 2(*e*), wound around the vacuum chamber, built with some length of available electric cable. The two PFExt nearer to the equatorial plane carried a current in the toroidal direction opposite to the plasma current winding inside the plasma centerpost: therefore the vertical field had the right effect of containing the expansive force of the plasma torus. Furthermore the current flowed inside the equatorial PFExt coils in the direction opposite to the current flowing inside the internal PF2\PF3 mirror coils and matched the requirement of interfacing oppositely directed B field in order to trigger magnetic reconnections. The two other PFExt coils in figure 2(*e*), the ones farthest from the equatorial plane, were used only for correcting the displacement effect that the equatorial PFExt coils had on the positions of the two plasma "mushrooms" in front of both electrodes, shown in figure 1(*c*). The quasi-stationary DC electric potential difference required between the electrodes (along the 2.10 m long magnetic lines of force) was only 220 V for sustaining in Hydrogen the centerpost discharge alone, but rised to 240 V for maintaining in addition the "lean" tori.

In the second Phase-2 of the experiment the tori will be shaped not anymore in the form of "lean" tori, but of "spherical" tori, i.e. "apples with thinly perforated cores": the plasma confinement properties improve with the increase of the current flowing inside the torus, so it is indeed expedient to fatten the torus and to restrict the centerpost, as much as possible.

In the Phase-2 of the experiment, the total number of cathode Tungsten filaments will grow by a factor of 7, from 54 to a total of 378, alongside with the plasma centerpost current, which will increase from 10 kA to 70 kA; the expected "spherical" shaping should allow (Micozzi et al. 2010) for up to 300 kA of toroidal plasma current to flow inside the spherical tori that will be sustained for up to 1 sec.

3. Insulation of anode gas feeding system by Teflon components

A preliminary campaign of experiments on PROTO-SPHERA was run from the summer of 2014 up to February 2015, dedicated to the plasma break-down. In this phase the plasma central discharge was obtained in presence of the final annular cathode on the bottom of the machine, but with a simple provisional cylindrical anode on top of it.

Eventually in May 2015 the final annular anode, enclosed within the upper mechanical group, was lowered on top of the Aluminium cylindrical vacuum vessel, see figure 3(*a*). Just at this time the first use of plastic insulators began: the annular anode gas-puffing system had to be electrically insulated from the AISI 304 top lid of the machine; Teflon blocks and Teflon tubes for injecting gas on the rear of each of the 30 annular anode modules were introduced, see figure 3(*b*). Since then the experiment has been run for about 4 years without any damage to these Teflon components .

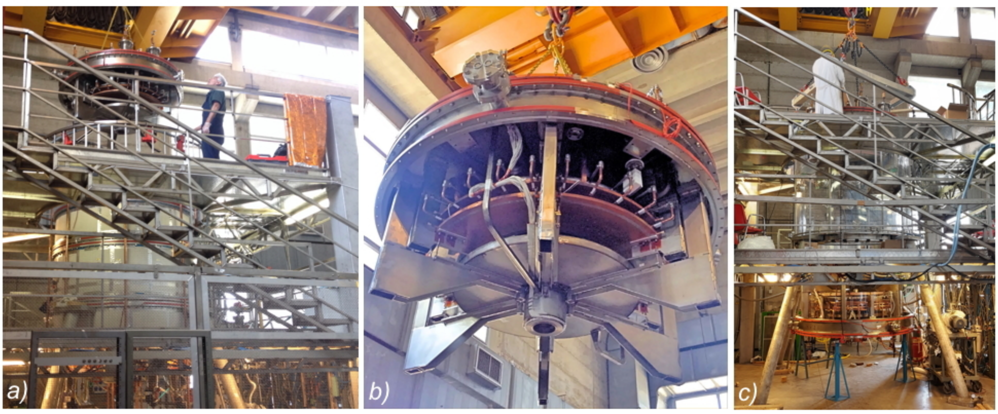

FIGURE 3. (*a*) The annular anode being lowered on the Aluminium vacuum vessel (year 2015). (*b*) Enlarged image of the anode, on the rear side of which white Teflon blocks and tubes insulate the gas-puffing system from the upper lid. (*c*) The annular cathode, below the machine, being lifted into the new PMMA transparent vacuum vessel (since year 2019).

Figure 3(*c*) illustrates one of the lifting of the lower cathodic mechanical group from the bottom of the machine at a much later date (2019), showing that the cylindrical geometry is quite suitable for all kind of interventions, repairs and corrections. During the years from 2014 to 2019 the experiment was opened for corrections: 7 times the upper mechanical group and 5 times the lower mechanical group were removed and reinserted. This possibility of easily opening, correcting and closing the machine, is the unique feature that has allowed for the progressive adjustment of the boundary conditions of the experiment.

4. Magnetic nozzle insulation by large Polycarbonate top & bottom flanges

The Phase-1 operation of PROTO-SPHERA began during the year 2015, in presence of the final annular anode. In October 2015, the centerpost current reached I_e=3.0 kA in Argon plasmas and lasted only 0.3 s. A number of problems still prevented the achievement of the full current of 10 kA, the full duration of 1 sec and even the successful production of any Hydrogen plasma centerpost. The first problem was an increasing level of metallization deposited by the plasma on the Copper busbars (figure 4(*a*)) that, penetrating through the top and the bottom lids, introduce inside the vacuum vessel the current that the electrodes convert into plasma centerpost current.

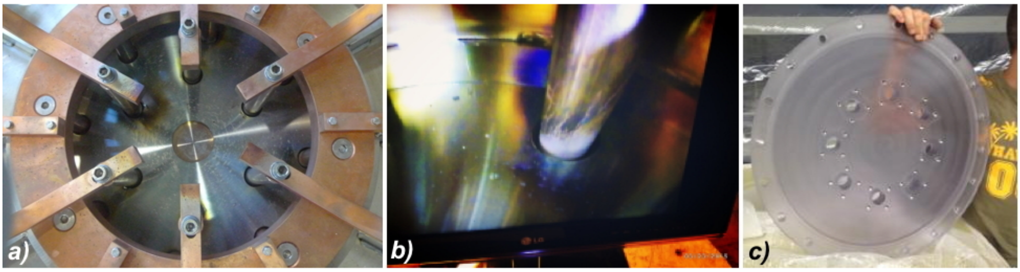

FIGURE 4. (*a*) Anode top busbars viewed from inside the vessel. (*b*) One of the cathode bottom busbar viewed also from the inside, both in presence of AISI304 central lid flanges. (*c*) Large new anodic polycarbonate top lid flange.

The busbars went through two big AISI304 flanges, placed in the center of the upper and the lower lid of the machine, the spaces available for their insulation were quite narrow, see figure 4(*b*): this made the plasma operations increasingly difficult. The two metal flanges for the busbars penetration inside the vacuum were then replaced by two 4 cm thick polycarbonate insulating flanges (figure 4(*c*)), machined with the same mechanical details as the metal ones. This replacement happened in June\July 2016.

4.1. *Triple magnetic X-points and magnetic nozzles*

But the problem with the top and bottom busbars was not only one of electrical insulation, it was a direct effect of the physics upon which the experiment is based: one of the appealing features of configuration similar to PROTO-SPHERA for future magnetic confinement thermonuclear reactors, is that they will contain open field lines also and that they will be endowed with two degenerate (or triple) X-points (with null field, B=0), placed on the symmetry axis, roughly in the middle the two opposite annular electrodes.

One of the two triple X-points (Tuszewski 1988), the upper one illustrated in the field map of figure 5(*a*), is already observable in PROTO-SPHERA and shown in figure 5(*b*) in the middle of the anode (figure 5(*c*)), while the plasma is still present but the centerpost discharge is being switched-off. It is quite evident from figure 5(*b*) that the triple X-points channel plasma directly upon the flanges placed in the center of the upper and lower lid of the machine. The strong light emitted from the hot cathode filaments does not allow the observation of the opposite lower cathodic triple X-point.

FIGURE 5. (a) Poloidal cross section map of magnetic lines of force near the anode (yellow), showing the triple X-point on axis, in the middle of the anodic PFInt-B coils (blue). (*b*) Image of the upper triple X-point, while the plasma centerpost (which lays below) is still present but is being switched-off, shot #117. (*c*) The hollow annular anode.

In a future fusion reactor the high energy and large poloidal Larmor radius charged fusion products will drift across the magnetic separatrix, shown in figure 1(*b*), from the nuclear burning torus into the open field lines of the plasma centerpost; their expulsion from the plasma centerpost will be preferentially from one of the two triple X-points (Rogier 2003), depending upon the sign of $\vec{\boldsymbol{j}} \bullet \vec{\boldsymbol{B}}$ inside the plasma. This preferential triple X-point could become the first component of a magnetic nozzle, allowing for the use of the nuclear fusion burner as a space thruster, whereas the depressed triple X-point could be used for direct energy conversion.

Thanks to the polycarbonate flanges the metallization problem has been solved on both electrodes and more than 1200 plasma discharges, like the ones shown in figure 6(*a*) and 6(*b*), have thereafter been obtained, without any further deterioration caused by any of the two triple X-points.

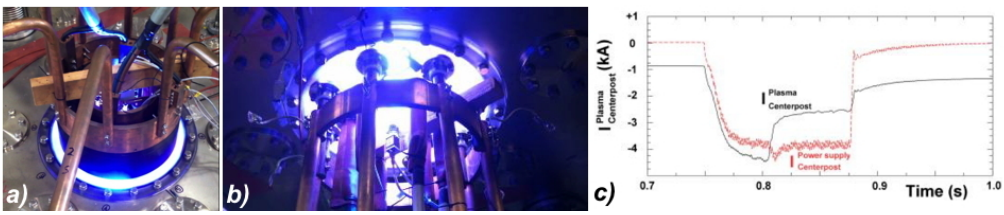

FIGURE 6. (*a*) The visible light of an Argon plasma centerpost emerging from the upper anodic polycarbonate flange, shot #567. (*b*) The visible light of an Argon plasma centerpost emerging from the lower cathodic polycarbonate flange, shot #577. (*c*) Waveforms of Argon centerpost plasma current, evidencing a sudden decrease after the centerpost discharge becomes attached to the Aluminium cylindrical vacuum vessel, shot #208.

A remaining problem was the one of spurious discharges, that drove plasma currents from the anode top busbars to the Aluminium cylindrical vessel and from it to the cathode bottom busbars. In Argon these spurious current paths were not strong enough such as to trigger abrupt plasma terminations, their effect was limited to sudden decreases of the plasma centerpost current, an example of which is shown in figure 6(c); the sudden current drops were in all cases associated with the plasma centerpost discharge becoming attached to the conducting Aluminium vacuum vessel.

5. Lining with a polycarbonate foil the Aluminium vacuum vessel

The Aluminium conducting vacuum vessel acted therefore as an unwanted current bridge, in parallel and in competition with the plasma centerpost current I_e (figure 7(*a*)). In Hydrogen plasmas the unwanted current paths were so strong as to lead to plasma terminations, an example of which is shown in figure 7(*b*) and 7(*c*), the termination phenomenon was not so different from the well-known Tokamak disruption (Boozer 2012). The Hydrogen plasma is much more prone to terminations than the Argon plasma as the initial break-down voltage (over a total distance of 2.1 m along the magnetic field lines) can be as low as 80 V for an Argon plasma but triples to 240 V for a Hydrogen plasma.

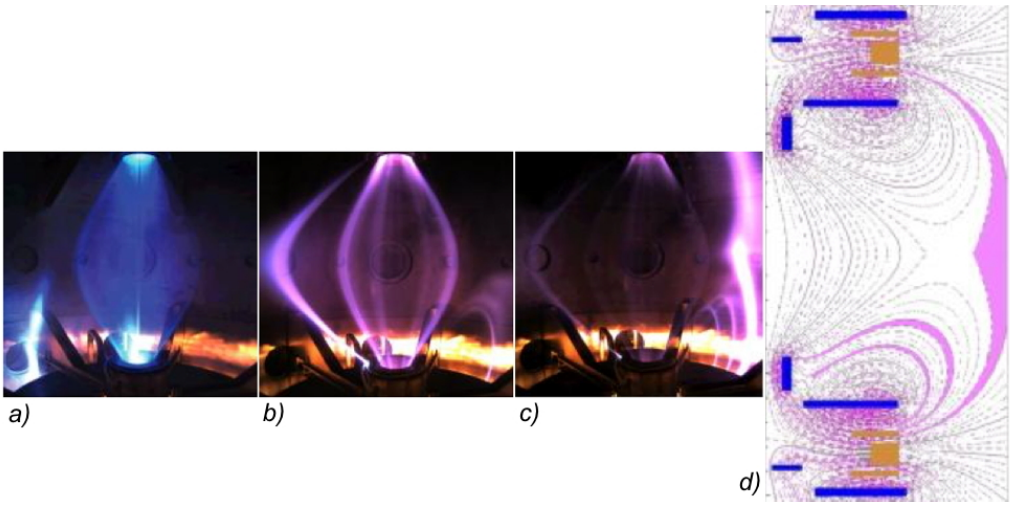

FIGURE 7. Spurious current path in presence of the Aluminium vacuum vessel: (*a*) Argon centerpost partially affected, shot #128; (*b*) Hydrogen centerpost seriously affected, shot #78; (*c*) Hydrogen centerpost driven to plasma termination on sub-millisecond timescale. (*d*) Maps of magnetic field with spurious current paths being evidenced.

This problem was solved in December 2016, by lining the inner side of the Aluminium vacuum cylinder with two, doubly overlapping, 2 mm thick, 2.05 m high, about 6.4 m overall circumference, large polycarbonate foils (figure 8(*a*)). The two polycarbonate foils were however lining the 2 m high Aluminium cylinder only and could not but leave uncovered the two AISI304 top and bottom ferrules, as shown in figure 8(*b*). Because of this constraint two secondary, again doubly overlapping, polycarbonate linings, also 2 mm thick, were added on the rear of the upper anodic mechanical group, figure 8(*b*), and on the rear of the lower cathodic mechanical group, figure 8(*c*).

All phenomena of attachment of the centerpost plasma to the wall vanished, and no plasma termination was never ever observed since then. But, nevertheless the polycarbonate linings, the Argon plasma centerpost current was not yet able to overcome I_e=3.5 kA: after this current level a slower current decay appeared, as shown in figure 9(*a*); the reason was again the presence of residual plasma currents flowing outside the proper centerpost path.

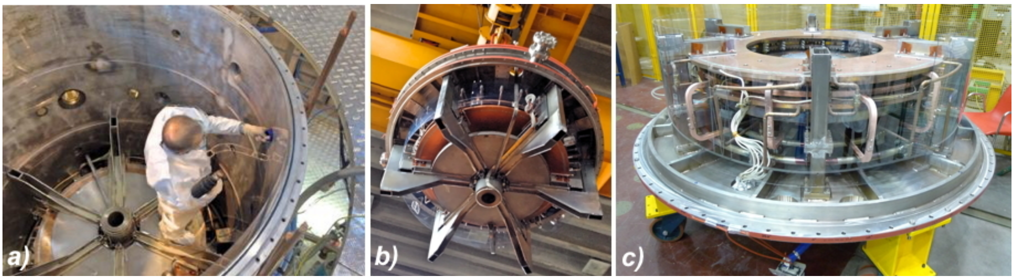

FIGURE 8. a) The Aluminium vessel being lined on its inner wall, by two, doubly overlapping, 2mm thick polycarbonate cylindrical foils. b) Similar doubly overlapping foils surround the upper anodic mechanical group. c) Same for the lower cathodic mechanical group.

These spurious plasma currents were however not anymore forming large cross section paths (as in figure 7), but they took the shape of thin current carrying plasma filaments, emerging from the lower (cathodic) PF2 mirror coil, as shown in figures 9(*b*) and 9(*c*); the filaments were usually brighter on their plasma-metal terminations at their negative electric potential but almost invisible on their plasma-metal terminations at their positive potential.

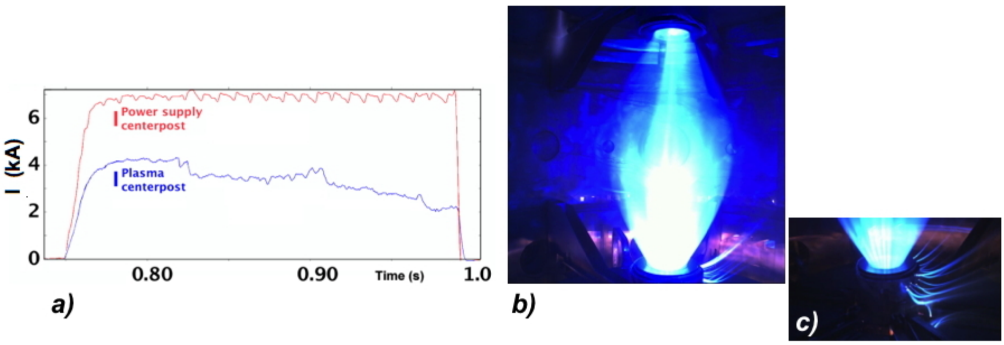

FIGURE 9. (*a*) Waveforms of Argon centerpost plasma current, evidencing a slow decrease of plasma centerpost current I_e. (*b*) and (*c*) Spurious plasma currents with filamentary patterns near the lower PF2 mirror coil. All figures refer to shot #597.

Like in the case of ELM instabilities (Kirk 2005), the filaments follow closely the magnetic lines of force and significantly break the axial symmetry of the machine.

6. Polycarbonate diaphragms and spacer insulating rings to fulfill the aims of Phase-1

To prevent the flowing of plasma currents outside the prescribed path, two large insulating diaphragm separators, see figure 10, made out of a 10 mm thick polycarbonate slab, pierced by two holes for the plasma, were inserted in the year 2017 in the central part the machine, attached to edges of the upper and of the lower mechanical groups, not far from the two PF2 internal mirror coil, that are separated from each other by 0.87 m.

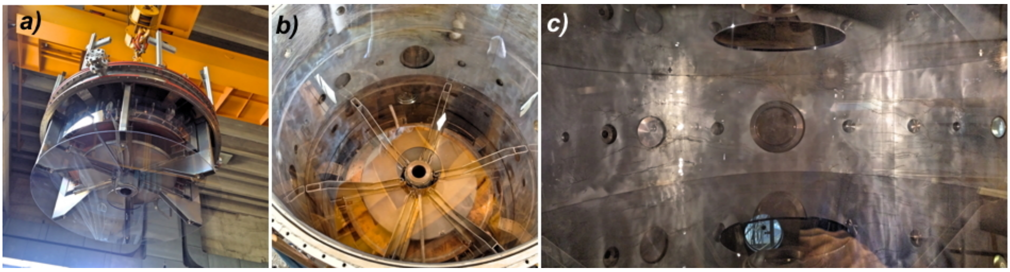

FIGURE 10. (*a*) Insulating diaphragm separator pierced by a hole near the upper PF2 mirror coil. (*b*) Same for lower PF2 mirror coil. (*c*) Empty region for the main plasma, near to the machine's equator, limited by the two diaphragm separators.

Furthermore, to avoid that any plasma current could still connect the anode top busbars to the AISI304 upper ferrule and, flowing through the Aluminium vessel, connect the AISI304 lower ferrule to the cathode bottom busbars of the machine, a polycarbonate insulating spacer ring, vacuum sealed with two o-rings on both sides, was inserted between the upper ferrule and the Aluminium vessel, as figures 11(*a*) and 11(*b*) show; on the bottom part of the machine an identical insulating spacer ring was put in position.

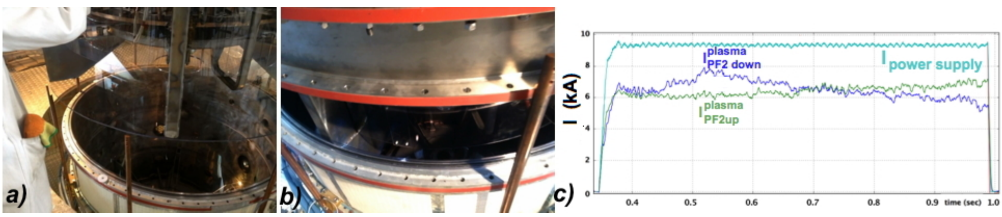

FIGURE 11. (*a*) and (*b*) The machine's upper group entering with the diaphragm head-on into the 2mm thick polycarbonate cylindrical foil that lines the Aluminium vessel, the upper spacer ring being held in position. (*c*) Waveforms of Argon centerpost plasma current I_e reaching 7 kA, after diaphragms and spacer rings were introduced, shot #614.

The Polycarbonate diaphragms and the spacer insulating rings allowed the sustainment of the Argon Plasma Centerpost at 7 kA current level, for 0.7 sec long discharges, illustrated in figure 11(*c*). Some spurious plasma current still sneaked through the narrow clearance (1-2 mm) existing between the large polycarbonate foil lining the inside of the cylindrical Aluminium vessel and each of the two diaphragms. In December 2017, therefore the two diaphragms were detached from the upper and the lower mechanical groups and glued instead, as shown figure 12(*a*), to the cylindrical large polycarbonate foil, with a vacuum compatible strong sealant able to sustain their weights. This last modification has allowed in January 2018 the attainment of the full current deliverable by the existing arc discharge power supply: 10 kA in Argon, as well as in Hydrogen (figure 12(*b*) and 12(*c*)). The anode-cathode voltage difference increased in Argon from 120 V at break-down up to 190 V in the discharge flat-top, whereas in Hydrogen it decreased from 240 to 220 V. In Hydrogen the current-voltage characteristic was that of a standard arc discharge, whereas in Argon multiple ionizations made the current-voltage characteristic look somewhat different. The aims of Phase-1 of the PROTO-SPHERA experiment (10 kA Plasma Centerpost in Hydrogen) had therefore been fulfilled. Only after the corrections to the boundary conditions of the experiment, introduced through a variety of insulating materials, it became possible to obtain a 1 sec lasting Centerpost Hydrogen plasma and it is remarkable that the plasma current I_e was then immediately produced at the full level of 10 kA.

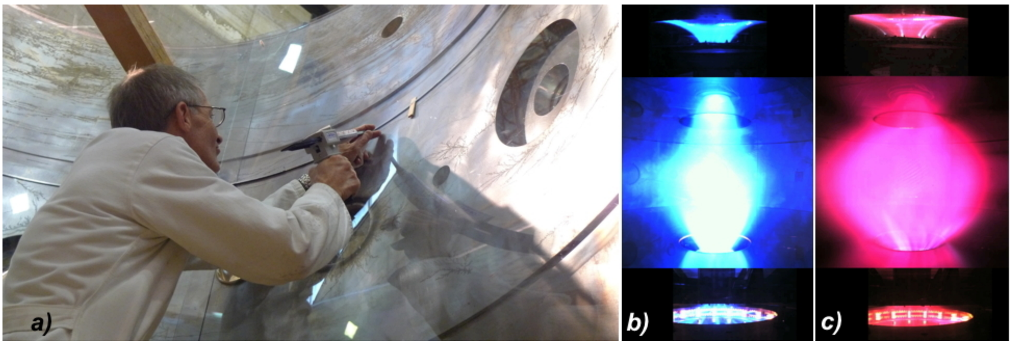

FIGURE 12. (*a*) Upper diaphragm being glued to the cylindrical large polycarbonate foil with a vacuum compatible strong sealant, able to sustain its weight. (*b*) Centerpost discharge at full current I_e=10 kA in Argon, shot #954. (*c*) Centerpost discharge at full current I_e=10 kA in Hydrogen, shot #969.

At the end of Phase-1 all the issues about the boundary conditions and the problems of insulation appeared to have been solved, as far as the plasma centerpost only plasma discharges were concerned. But moving beyond Phase-1 and attempting to produce the first plasma tori around the plasma centerpost, introduced new issues with the boundary conditions and reopened a few insulation problems, already solved in Phase-1.

7. First Tori and the effect of their magnetic separatrices

In April 2018, a couple of months after having fulfilled the Phase-1 objectives, PROTO-SPHERA also produced and sustained the first Hydrogen plasma tori, able to carry a toroidal current up to 7 kA. This was obtained by adding 4 impromptu magnetic vertical field coils (the PFExt of figure 1(*d*)) wound around the vacuum chamber, fed in series with the PFInt-B internal coils; but nothing else was changed inside the machine, not even the vacuum was broken. The tori were successfully obtained: they were extremely "lean", as expected from plasma magnetic predictive equilibrium calculations that included the PFExt coils effect, but they were unexpectedly strongly up/down asymmetric, see figure 13(*a*). The skin-current effect of the 4 cm thick Aluminium vacuum vessel delayed by 0.6 s the penetration of the PFExt vertical magnetic field inside the machine; therefore the plasma tori were produced starting from 0.6 s, in the purely magnetostatic field, obtained after the skin current flowing in the Aluminium cylinder was dissipated, so their sustainment was limited to about ½ s. The tori were always equipped with a "magnetic separatrix", i.e. a conical "fan" of plasma able to discharge the power dissipated inside the torus, coming out of the two circles of ordinary magnetic X-points (B_{pol}=0, B_T≠0). The filamentation of the plasma current, when it emerged from the lower PF2 internal mirror coil, was very intense, see figure 13(*b*). The impact on the lower diaphragm, see figure 13(*c*), did clearly evidence the nearly axisymmetric nature of the plasma tori, but the lower polycarbonate diaphragm unfortunately acted as an inappropriate divertor plate for the magnetic separatrix.

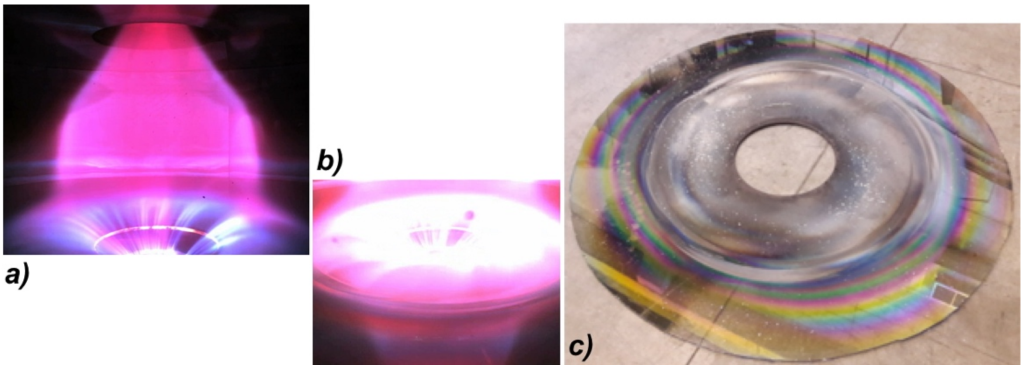

FIGURE 13. (*a*) "Lean" torus visible as a brighter belt at the outer edge of the Hydrogen plasma centerpost. (*b*) Lower magnetic separatrix, just below the lower circle of X points, from a different camera. Both from shot #1202. (*c*) Polycarbonate lower diaphragm, removed at the end of the experimental campaign in which PROTO-SPHERA produced the first plasma tori.

7.1. *The conical divertor plate and the problem of current filamentation*

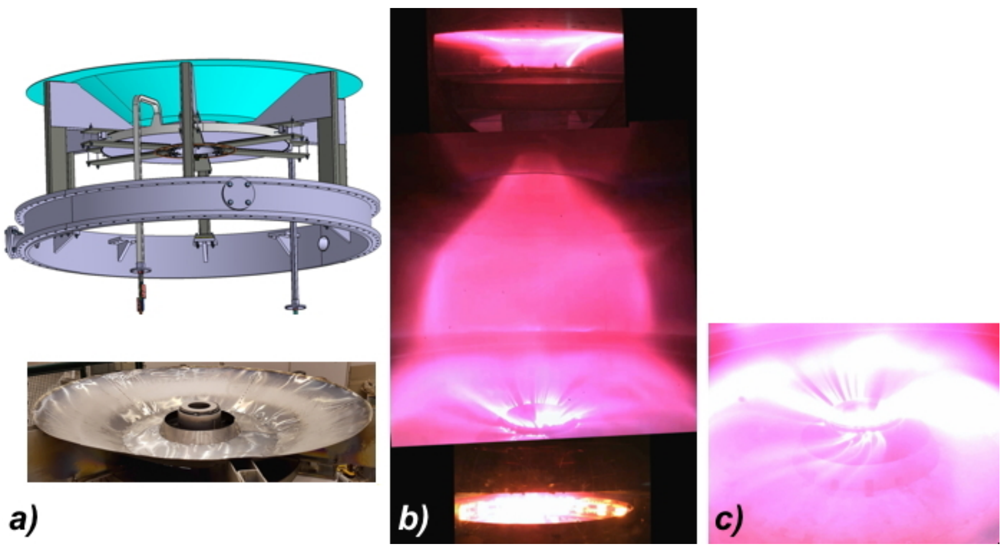

FIGURE 14. (*a*) CAD design of conical lower divertor plate (top) and the first 0.5 mm thick AISI304 provisional lower divertor plate (bottom). (*b*) "Lean" torus visible as a brighter belt at the outer edge of the Hydrogen plasma centerpost, shot #1280. (*c*) Lower magnetic separatrix, just below the lower circle of X points, from a different camera, same shot.

In June 2018 the first provisional lower conical divertor plate, sketched in figure 14(*a*), was added to the experimental machine, as a home-produced portion of cone in 0.5 mm thick AISI304, see figure 14(*b*). The central holes pierced inside each of the two insulating polycarbonate diaphragms were furthermore enlarged up to an internal diameter of 400 mm. Figures 14(*b*) and 14(*c*) show that a rebalancing of the main equatorial plasma was obtained, as the new presence of a weak upper divertor fan illustrates, along with a decrease of the up/down asymmetry in the separatrix and with a slight weakening of the filamentation of the plasma current, when it emerged from the lower PF2 internal mirror coil.

However the two large insulating diaphragm separators of Phase-1 still had too narrow holes at their center, clearly incompatible with the extent of the magnetic separatrix, while the filamentation of the plasma emerging from the lower PF2 had resurfaced as a relevant problem. Unpleasant effects for the plasma tori are associated with any kind of filamentation of the plasma current: the plasma filaments act as a relevant source of magnetic disturbances to the overall axial symmetry of the magnetic configuration. The two main disturbances from current carrying filaments are: a) to add a counterflowing current on the outboard edge of the torus and b) to introduce an ergodic component to the magnetic field inside the torus (Alladio 2008). The results would be that: a) the filamentation could therefore contrast the Helicity Injection and b) the integrity of the magnetic toroidal flux surfaces could be spoiled. Both points could worsen the energy confinement inside the plasma tori in the future Phase-2 of the experiment: the first point could decrease the toroidal current in the spherical torus I_{ST}, by decreasing the current ratio I_{ST}/I_e; the second point could directly enhance the energy losses through an ergodic magnetic field.

8. PROTO-SPHERA rebuilt for the intermediate Phase-1.5, trying the first spherical tori

In order to move towards the Phase-2 of PROTO-SPHERA it was decided to operate in 2019-2020 an intermediate Phase-1.5, having the aim of progressively pushing the plasma from the "lean" tori of Phase-1 to the spherical tori of Phase-2.

8.1. *The new first set of compression coils and their insulations*

A reduced-current version of the PFInt-A compression coils, shown in figures 15(*a*) and 15(*b*), was home-manufactured and inserted inside the machine during the summer of 2019: it was a group of 6 coils, all fed in series, earlier not present in the experiment. Four of the PFInt-A coils were contained inside two new (industrially built) 2 mm thick AISI304 conical divertor plates, on their plasma-facing sides. Two new large Teflon diaphragms were interposed between each of the two AISI304 conical divertor plates and its nearest electrode, the lower one is shown in figure 15(*c*). The two other PFInt-A coils were wound between the rear of each conical divertor plate and its nearby Teflon diaphragm. The innermost part of each Teflon diaphragm, being the nearest to the plasma, was protected by two massive Alumina cones, the lower one is shown in figure 15(*d*).

The new home-manufactured PFInt-A coils were not enclosed into full casings and had a similar geometry, but a reduced number of turns, with respect to the final armored PFInt-A coils, that are planned to be industrially built for the Phase-2 of the experiment.

FIGURE 15. The new six PFInt-A compression coils: (*a*) Two within the upper conical divertor plate and one above it; (*b*) Two within the lower conical plate and one below it. The green fiberglass blocks insulate the horizontal supports holding the compression coils from the vertical sustaning columns. (*c*) The new upper conical 2 mm thick AISI304 divertor plate, seen from above; below it the large Teflon diaphragm. (*d*) The large Teflon diaphragm viewed from below, showing the inner Alumina cone that surrounds the hole inside the lower PF2 mirror coil.

The present intermediate Phase-1.5 of the machine aims therefore at producing plasmas as similar as possible to the Phase-2 plasmas, albeit at much lower currents. Before increasing by a factor of 7 the electrode-driven current in the plasma centerpost it is mandatory to operate successfully the intermediate Phase-1.5 of the machine: the aim is, in presence of spherical tori, to learn about the DC voltage that will be required between electrodes, about the efficiency of Helicity Injection I_{ST}/I_e and to mend all the resurfaced insulation problems.

8.2. *The new insulating and transparent cylindrical vacuum vessel*

In order to remove the electrical conductivity in the cylinder enclosing the experiment, a new insulating cylindrical vacuum vessel was designed and then commissioned to an industrial firm. The new insulating vessel was chosen not only in order to solve a variety of insulation problems, but in order to remove as well the skin current effect of the conductive Aluminium vessel, allowing for the sustainment of the centerpost + torus plasma to reach the full 1.1 s, the maximal duration deliverable by the power supply.

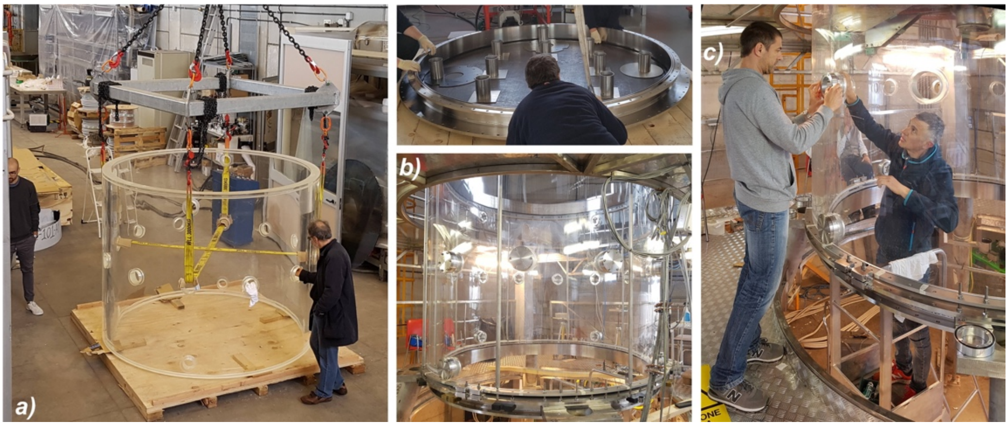

FIGURE 16. (*a*) The 9 cm thick, 2 m internal diameter, 1.7 m high, new PMMA vessel. (*b*) One of the two new AISI304 ferrules being tested upon a 10 mm thick Viton flat gasket (top). The new vessel placed in position, with the Viton flat gasket interfacing it with the new bottom ferrule, held by the sustaining legs, pre-charged by compression poles and aligned by brackets (bottom). (*c*) Closing the diagnostic ports by "bulkhead fitting" technology.

The only suitable material for producing a 1.7 m high and 2 m internal diameter insulating cylinder turned out to be PMMA (poly-methyl-metacrylate). The thickness of the PMMA wall, albeit originally designed to be 5 cm, was almost doubled by the producing industrial firm to 9 cm (figure. 16(*a*)).

Two additional AISI304 ferrules, each 0.15 m high, were built and introduced at the two edges of the cylinder to allow for maintaining in use the four pre-existing supporting legs of the machine. The legs were connected to the experiment at a different connection height; figures 3(*a*) (before the PMMA vessel) and 3(*c*) (after it) show that the vacuum vessel bottom lid was consequently displaced upwards by about 40 cm. Two Viton flat gaskets, 10 mm thick and with shore75 hardness, shown undergoing test on the top of figure 16(*b*), have been used as vacuum fitting interfaces between the two flat edges of the PMMA cylinder and the new ferrules: such a choice was compelled by the limits of planarity of the PMMA cylinder's edges, which could be manufactured only within 3 mm of overall planarity tolerance. The 30 plus Tons of force exerted under vacuum on each of the two Viton flat gaskets were more than enough to held the vacuum. However, in order to ease the beginning of the vacuum pumping, a force of about 15 Tons was pre-charged upon the two gaskets, by compression poles anchored on the two new ferrules. Alignement brackets were introduced, in order to clamp the two new ferrules to the two grooves carved near the edge of the PMMA cylinder. All those auxiliary components are visible on the bottom of figure 16(*b*) and in figure 16(*c*).

Altough the PMMA material is almost perfectly transparent to visible light and to UV light (no UV-filtering surface treatment was performed on the purchased PMMA cylinder), the light in the Infrared spectrum, as well as in the soft-X ray spectrum, gets absorbed; furthermore the 9 cm thick wall, which has a limited tolerance in its overall cylindrical finishing, introduces random refractory behaviours, which are better avoided for diagnosing the plasma. The PMMA vessel was then carved, on the equatorial plane, by twelve 100 mm diameter diagnostic ports for observing the main plasma and by four upper and four lower

70 mm diameter ports, centered 150 mm far from the PMMA cylinder's edges, for diagnosing the anodic and the cathodic plasmas. To avoid possible cracks, no further threaded holes could be carved in the PMMA vessel near the diagnostic ports, therefore it was not possible to simply screw ordinary flanges to the PMMA vessel in order to close the vacuum. The PMMA material was instead accurately parallel flattened near each port, on both sides. Then the "bulkhead fitting" technology was used, based on an outer o-ring pressed by tensioning rods inserted between the two flattened sides of the PMMA wall, as it is shown in figure 16(*d*); so the PMMA cylinder finally got its 20 diagnostic ports.

The inner side of the PMMA cylidrical wall was at the end lined, once again, with two, dubly overlapping, 2 mm thick, 2.05 m high, about 6.4 m overall circumference, large polycarbonate foils, which serve the purpose of protecting the inner PMMA wall from any direct plasma effect and which screen the UV light emitted by the plasma: the UV light can be a hazard for the health of nearby people when the plasma is produced and would also degrade the transparency of the PMMA vessel.

From the point of view of the vacuum performances the new PMMA vessel was even better than the old Aluminium one: a base pressure of $6 \cdot 10^{-5}$ mbar was achieved after two weeks in the first round of vacuum pumping; this is more than enough, as the plasma is obtained at a filling gas pressure of about 10^{-2}-10^{-1} mbar; on the other hand the base pressure is clearly limited by more than 5 tons of various components contained inside the 8 cubic meters of the internal volume of the machine. After the first plasmas were produced inside the PMMA vessel, in the following rounds of opening and closing of the machine, an acceptable vacuum was recovered in a much shorter period of time: only 2-3 days after closing the machine.

8.3. *The new insertable and extractable polycarbonate diaphragms*

The two large insulating diaphragm separators, made out of a 10 mm thick polycarbonate slab, had to be completely rebuilt as well. Their internal holes were enlarged to a diameter of 1500 mm, as figure 17(*a*) and 17(*b*) show, and they were not anymore glued to the cylindrical large polycarbonate foil, but they reverted to be fixed to the anodic and cathodic mechanical groups.

In order to avoid that spurious plasma currents could sneak through the narrow outermost clearance (1-2 mm) between the polycarbonate diaphragms and the large polycarbonate foil lining the inside of the PMMA vessel, a foldable 3 mm thick Norseal red Silicon gasket, with shore30 hardness, was glued to each diaphragm and held in position by a further polycarbonate lining 2 mm thick, that appears on top of figure 17(*b*). The two mechanical groups were successfully inserted, as figure 17(*c*) shows, into the large, doubly overlapping, polycarbonate foils lining the inside of the PMMA vessel, (and later successfully extracted from it): both Silicon gaskets were able to fold (and unfold) properly, guaranteeing a reusable sealing, hermetic to any spurious plasma current sneaking in.

Unluckily an empty space of about 2 cm was instead left open between each polycarbonate diaphragm and its nearby AISI304 conical divertor plate, figure 17(*a*): the vain hope was that spurious plasma currents would not bend around both the diaphragm separators as well as around the conical divertor plates, but this was not a correct guess.

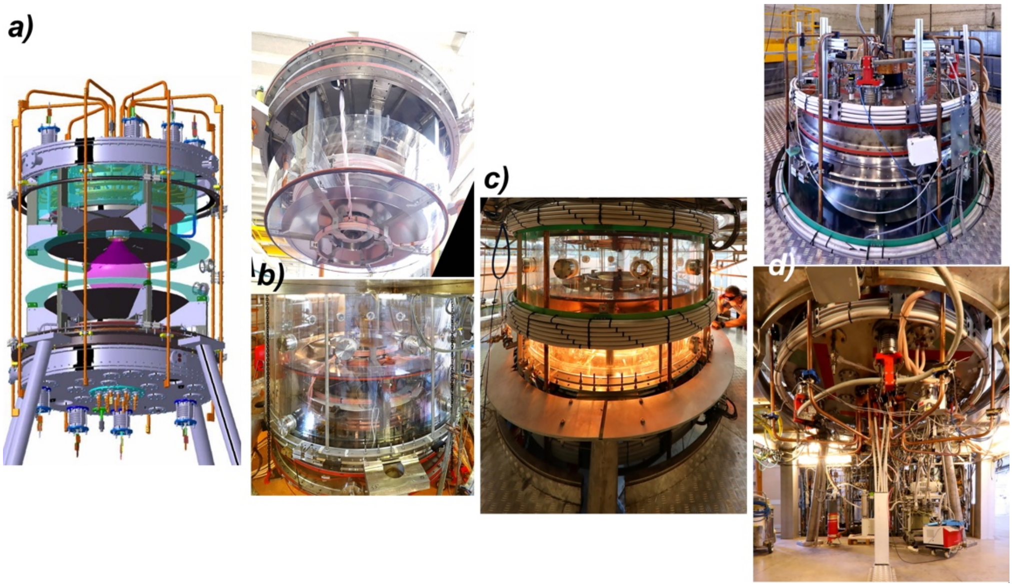

FIGURE 17. (*a*) CAD design of PROTO-SPHERA, rebuilt for Phase-1.5: plasma (pink), diaphragms (semitransparent green) and conical divertor plates (black). (*b*) Transparent diaphragm and foldable 3 mm thick red Silicon gasket at the edge of the upper mechanical group (top). Lower mechanical group, inserted into the PMMA vessel, with folded red Silicon gasket (bottom). (*c*) New external coils PFExt (grey), near the equator of the experimental machine and in presence of hot cathode filaments. (*d*) Upper and lower PFExt coils.

8.4. *The new external poloidal field coils*

The external poloidal field compression coils PFExt were also rebuilt with cables of much larger cross section than the ones used in 2018. Therefore in 2019 PROTO-SPHERA was endowed with 18 poloidal field coils (PF), divided in 3 sets: the 8 internal PFInt-B shaping coils, the original armored ones, shown in the CAD design of figure 1(*a*), the 6 new internal PFInt-A compression coils, illustrated in figures 15(*a*) and 15(*b*) and the 4 external PFExt coils, shown in figures 17(*c*) and 17(*d*). This has allowed, with the two existing PF coils power supplies, either to feed independently PFInt-B and PFExt coils, or independently PFInt-B and PFInt-A coils or even to feed independently PFInt-A coils and the series of PFInt-B and PFExt coils. In its final Phase-2 the experiment will have a third additional PF coils power supply, so that it will be possible to feed independently all the 3 sets of coils.

9. PROTO-SPHERA in Phase-1.5: first results and further corrections

9.1. *The "lean"tori lasting for 1 s, in absence of any surrounding conductor*

The Hydrogen "lean" tori, already obtained in the year 2018, were produced again in the autumn of year 2019, and with the same recipe: i.e. using the external PFExt as the only compression coils. The new "lean" tori had identical characteristics and the same level of toroidal current as the ones of 2018, notwithstanding the absence of any metallic vacuum vessel surrounding the plasma; furthermore, just because of the absence of skin effects, in the 2019 plasma campaign the "lean" tori could be sustained for up to 1 sec.

9.2. *The first attempts to produce spherical tori in Argon and in Helium plasmas*

The first plasma operations of Phase-1.5, in which the new PFInt-A compression coils were energized (in presence or in absence of currents flowing in the external PFExt), gave reasonable results for Argon discharges, an example is shown in figure 18(*a*).

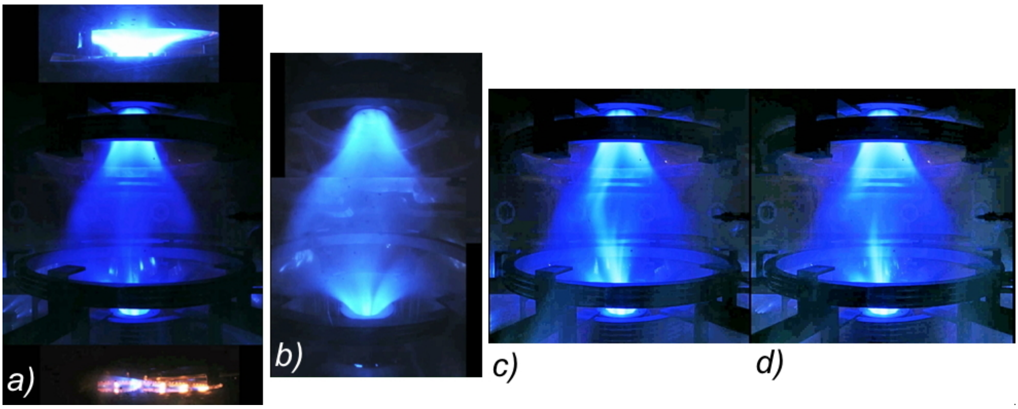

FIGURE 18. Shot #1687, Argon plasma with the PFInt-A compression coils energized. (*a*) Overall view (superposition of anodic, main and cathodic plasma images from 3 different cameras). (*b*) View of the main plasma, with distorted perspective, composed by images of two tilted cameras looking at the upper and at the lower PF2 mirror coils, from which the plasma centerpost emerges. (*c*) Spurious Argon currents, observed as low luminosity stripes in front of the lower PFInt-A coils. (d) Luminosity stripes at different positions for a later time-slice.

Plasma tori with an aspect ratio lower than the "lean" tori of 2018 were obtained, this time the plasma inside the tori became more transparent than the centerpost plasma, suggesting that the tori have a higher temperature than the centerpost, and furthermore they could be sustained for 1 sec. The filamentation of the plasma emerging from the lower (cathodic) PF2 internal mirror coil was usually absent or very limited, as shown in figure 18(*b*). However the empty space of about 2 cm left open between each polycarbonate diaphragm and its nearby AISI304 conical divertor plate, figure 17(*a*), allowed for the sneaking through of spurious Argon plasma currents, evident in figures 18(*c*) and 18(*d*). The spurious plasma currents bent around the polycarbonate diaphragms, in particular around the lower one. The horizontal supports holding the new PFInt-A compression coils were indeed insulated from the AISI304 vertical columns (sustaining the weight of the lower mechanical group) by fiberglass blocks near the empty space, as shown in Figure 15(*b*). The spurious plasma discharges were however able to jump over the insulating blocks and to attach directly to the supporting columns and to inflict to them some damage.

Also in Helium discharges, shown in figure 19, when the new PFInt-A compression coils were energized, the behaviour of the plasma was quite similar and produced tori with aspect ratio lower than the "lean" tori of 2018. The circles of X-points and the separatrix fans associated with the Helium tori, evident in figure 19(*a*), were much sharper than in

Argon plasmas (see figure 18(*a*)), but some filamentation of the plasma still emerged from the upper (cathodic) PF2 internal mirror coil, and is evident in figure 19(*b*); in Helium the up/down lack of symmetry was biased toward the upper side.

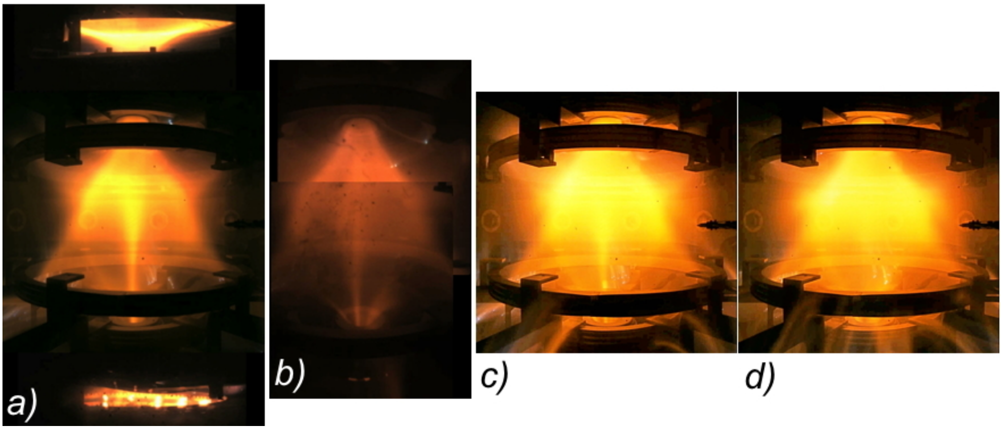

FIGURE 19. Shot #1752, Helium plasma with the PFInt-A compression coils energized. (*a*) Overall view (superposition of anodic, main and cathodic plasma images from 3 different cameras). (*b*) View of the main plasma, with distorted perspective, composed by 2 tilted images of cameras looking at the upper and at the lower PF2 mirror coils, from which the plasma emerges. (*c*) Spurious Helium plasma currents, observed as low luminosity stripes in front of the lower PFInt-A coils. (d) Luminosity stripes at different positions for a later time-slice.

The spurious filamented Helium plasma currents, clearly visible in figures 19(*c*) and 19(*d*), did bend as well around the lower polycarbonate diaphragm, just as in the Argon plasma. Because of the large spurious plasma currents, it was impossible to estimate the toroidal current contained either inside the Argon or inside the Helium tori.

9.3. *The first attempts to produce spherical tori in Hydrogen plasmas*

In Hydrogen, when the new PFInt-A compression coils were energized, the behaviour was still different, the plasma torus was not observed and may not even have been present, as shown in figure 20(*a*), maybe because of the too pronounced filamentation of the plasma emerging from the lower (cathodic) PF2 internal mirror coil, see figure 20(*b*), but at the same time the spurious Hydrogen plasma currents bending around the polycarbonate diaphragms were much less evident than in Argon or in Helium, see figures 20(*c*) and 20(*d*).

Furthermore during a 1 s discharge in Hydrogen the lower massive Alumina cone, that was shown in figure 15(*a*) and that surrounded the hole of the lower PF2/PF3 internal mirror coils, was broken in pieces by thermal stresses and fell down upon the lower PF4-1, the lowest-lying poloidal field coil among the PFInt-B shaping group. During the fall of the Alumina pieces the colour of the cathodic plasma turned blue, but the main plasma near the equator remained unperturbed, without any change in the colour of the emitted light. The plasma operations could be continued also after this accident. The upper Alumina cone was cracked as well by thermal stresses, but its pieces remained in place.

Even in presence of large distortions of the plasma shape, in particular when a too large compression field was imparted by the PFExt or PFInt-A coils, terminations of the plasma discharges were never observed. In all the 500 discharges produced in 2019 the plasma disappeared only when the DC voltage between electrodes was switched-off.

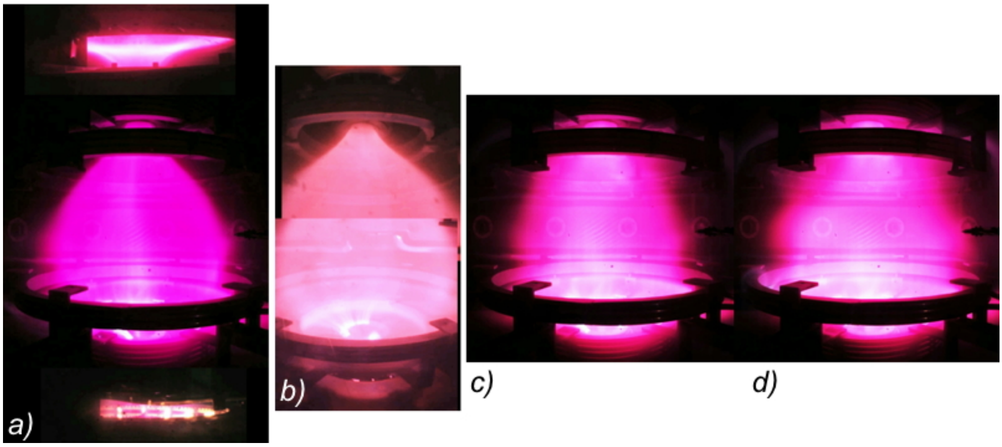

FIGURE 20. Shot #1683, Hydrogen plasma with the PFInt-A compression coils energized. (*a*) Overall view (superposition of anodic, main and cathodic plasma images from 3 different cameras). (*b*) View of main plasma, with distorted perspective, composed by 2 tilted images of cameras looking at the upper and at the lower PF2 mirror coils, from which the plasma emerges, evidencing filamentation. (*c*) Plasma filamentation near the PF2 coil and spurious Hydrogen plasma currents in front of the upper PFInt-A coils. (*d*) Same for a later time-slice.

9.4. *The actions for avoiding spurious plasma current paths*

In order to mend the two more relevant insulation problems, which appeared in the first plasma operation of Phase-1.5, a number of actions are presently underway.

The two broken massive Alumina cones, that surrounded the holes of each of the two PF2/PF3 internal mirror coils and protected each of them from their nearest electrode, will be replaced by two new AISI304 cones, which have been plasma sprayed with Alumina powder.

In order to hinder the spurious plasma currents bending around the diaphragms, whose damage is well illustrated by figure 21(*a*), two new polycarbonate diaphragms, with internal holes reduced from 1500 to 1060 mm, will be inserted. For the same purpose two new shore40 Silicon foldable gaskets are going to fill the empty spaces between each diaphragm and its nearby conical AISI304 divertor plate, in proximity of the polycarbonate internal lining of the vessel.

In order to avoid the filamentation of the plasma emerging from both of the PF2 internal mirror coils, shown in figure 20(*b*), and the consequent damages inflicted to the divertor plates, shown in figure 21(*a*), the open inner part of both AISI304 conical divertor plates (see figure 15(*c*)) is going to be closed by an additional AISI304 ring, overlapped by a hollow Teflon cap enclosing each PF2 coil, as illustrated in figure 21(*b*).

The six plus six horizontal supports holding the PFInt-A compression coils, shown in figure 21(*a*), are being rebuilt: starting from their outermost positions, near to the new shore40 Silicon foldable gasket, until their innermost position still covered by the polycarbonate diaphragm, they will be made out of fiberglass insulating material; only their innermost parts, which will come in contact with the plasma magnetic separatrix, will remain metallic.

In figure 21(*c*) it is shown that in the 2019 Argon plasma campaign, spurious discharges occurred between each of the back sides of the two AISI304 conical divertor plates and its nearest vacuum vessel lid, this was due to a mistake in the busbar connections which was promptly fixed. In order to avoid similar discharges in future, the two AISI304 conical divertor plates will remain metallic on their sides exposed to the plasma but will be sprayed by Teflon on their sides not facing the plasma.

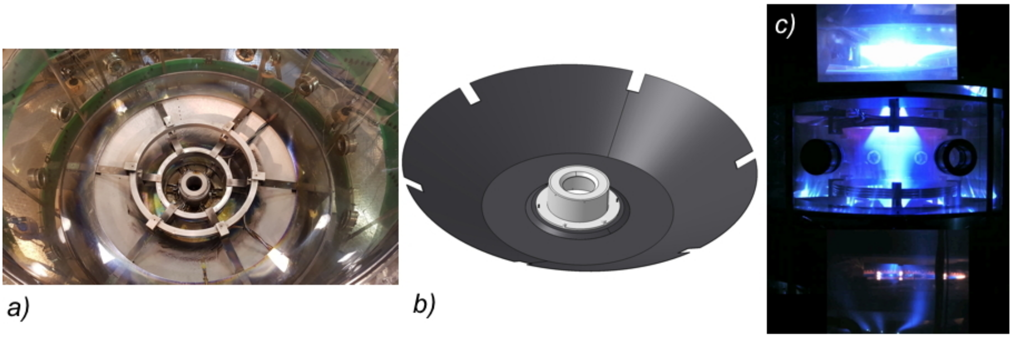

FIGURE 21. (*a*) Plasma induced metallization observed as darkening: of the innermost part of the lower conical divertor plate, due to filamentations of the plasma current near to the lower PF2 mirror coil; of the lower polycarbonate diaphragm, due to spurious plasma currents sneaking in the empty space left open between the diaphragm and its nearby divertor plate. (*b*) CAD design of the modified divertor plate (gray), closed by an AISI304 ring on the inner part and overlapped by a hollow Teflon cap (white), which will enclose the PF2 coil. (*c*) Shot #1556, Argon plasma with the PFInt-A compression coils energized: overall view (from 3 different camera images), evidencing spurious plasma discharges connecting each of the two metallic lids of the vacuum vessel to the back side of its nearest divertor plate.

10. Conclusions

The PROTO-SPHERA experiment, by removing the two metal central conductors of the Tokamak configuration and by replacing both of them with two electrodes feeding a plasma centerpost discharge, has overcome the need of a toroidal vacuum vessel for producing a magnetically confined plasma and has substituted it with a cylindrical chamber surrounding a simply connected plasma. The centerpost discharge is able, through magnetic reconnections (DC Helicity Injection), to form around itself and to sustain in steady state a plasma confining torus, which carries a steady toroidal current. The greatest difficulty in this new configuration is obviously the possibility that spurious plasma currents flow inside the cylindrical enclosure, but outside the proper centerpost route, along unpredicted and uncontrolled paths, hampering the magnetic configuration, reducing the efficiency by which the plasma centerpost injects magnetic helicity into the torus and finally making the field ergodic inside the torus.

In order to prevent the spurious plasma current paths, a number of corrections to the boundary conditions of the experiment have been carried out in its initial Phase-1 (centerpost only) and in its intermediate Phase-1.5 (first confined tori). All the electrostatic boundary corrections have introduced insulating materials inside the vacuum vessel in critical places near the plasma. Moreover the magnetic boundary conditions have been changed at the end of Phase-1, when the whole conducting Aluminium vacuum cylindrical chamber was replaced by the new insulating and transparent PMMA vacuum cylindrical vessel.

It is quite unconventional to have insulators near a plasma that investigates magnetic confinement in view of controlled nuclear fusion and even more an insulating vessel. The corrections have, step by step, not only achieved their desired results, without introducing problems of impurity contamination, but have also shown that the confined plasma tori of PROTO-SPHERA can be sustained in steady state (1 sec), without any need of stabilization by a massive shell-like nearby metal conductor. This is also a point of interest for laboratory simulations of astrophysical plasma phenomena, as all the astrophysical plasma events in the cosmos are bounded, after a given distance, by vacuum and therefore by one among the most effective electrical insulators.

REFERENCES

ALLADIO, F., GROSSO, L.A., MANCUSO, A., MANTOVANI, S., MICOZZI, P., APRUZZESE, G., BETTINALI, L., BURATTI, P., DE ANGELIS, R., GATTI, G., MONARI, G., PILLON, M., SIBIO, A., TILIA, B. & TUDISCO, O. (2000) Results of Proto-Pinch Testbench for the PROTO-SPHERA experiment. *Proc. of the 27th EPS Conference on Contr. Fusion and Plasma Phys. Budapest, 12-16 June 2000*, **ECA Vol. 24B**, 161-164

ALLADIO, F., MANCUSO, A., MICOZZI, P., PIERONI, L., ALESSANDRINI, C., APRUZZESE, G., BETTINALI, L., BURATTI, P., COLETTI, A., COSTA, P., CRESCENZI, C., CUCCHIARO, A., DE ANGELIS, R., FORTUNATO, T., FRIGIONE, D., GASPAROTTO, M., GATTI, G., GIOVAGNOLI, R., GROSSO, L.A., MADDALUNO, G., MAFFIA, G., MANTOVANI, S., MONARI, G., NARDI, C., PAPASTERGIOU, S, PILLON, M., PIZZUTO, A., ROCCELLA, M., ROGIER, F., SANTINELLI, M., SEMERARO, L., SIBIO, A., TILIA, B., TUDISCO, O., ZANNELLI, L. & ZANZA, V. (2001) PROTO-SPHERA. *ENEA, Serie Energia, Associazione Euratom-ENEA sulla Fusione,* **RT/ERG/FUS/2001/14**, ISSN: 1124-7932

ALLADIO, F., COSTA, P., MANCUSO, A., MICOZZI, P., PAPASTERGIOU, S. & ROGIER, F. (2006) Design of the PROTO-SPHERA experiment and of its first step (MULTI-PINCH). *Nucl. Fusion* **46**, S613–S624

ALLADIO, F., MANCUSO, A., MICOZZI, P. (2008) Rotating twisted filaments buoyancy: Comparison between the convective region of the sun and the edge of a tokamak plasma. *Plasma Physics and Controlled Fusion* **50**(12), 124019

BOOZER, A.H. (2012) Theory of tokamak disruptions. *Phys. Plasmas* **19**, 058101

BÜHLER, R. & BLANDFORD, R. (2014) The surprising Crab pulsar and its nebula: a review. *Rep. Prog. Phys.* **77**, 066901

CHEVALIER, R.A. (1982) Self-similar solutions for the interaction of stellar ejecta with an external medium. *Astrophysical Journal* **258**, 790-797

CORBIN, N. D. (1989) Aluminum Oxynitride Spinel: A Review. *Journal of the European Ceramic Society*, **Vol. 5**, pp. 143-154

FEAR, R.C., TRENCHI, L., COXON, J.C. & MILAN, S.E. (2017) How Much Flux Does a Flux Transfer Event Transfer? *Journal of Geophysical Research: Space Physics* **122**, 310–327

FEHLAU, P.E., CHAMBERS, W.H., FULLER, J.C., KUNZ, W.E., MILKEY R.W. & BLOCKER, N.K. (1971) Periodic Solar Flare X-ray Emission. *Nature* **232**, 42–43

HAVERKORT, J. W. & DE BLANK, H. J. (2012) Flow shear stabilization of rotating plasmas due to the Coriolis effect. *Physical Review E* **86**, 016411

HESTER, J.J, SCOWEN, P.A., SANKRIT, R., BURROWS, C.J., GALLAGHER-III, J.S., HOLTZMAN, J.A., Watson, A.M., TRAUGER, J.T., BALLESTER, G.E., CASERTANO, S., CLARKE, J.T., CRISP, D., Evans, R.W, GRIFFITHS, R.E., HOESSEL, J.G., KRIST, J.E., LYNDS, R., MOULD, J.R., O'NEILL Jr., E.J., STAPELFELDT, K.R. & WESTPHAL, J.A. (1995) WFPC2 Studies of the Crab Nebula. I. HST and ROSAT Imaging of the Synchrotron Nebula. *Astrophysical Journal* **448 (1)**. pp. 240-263

HESTER, J.J, STONE, J.M., SCOWEN, P.A., BYUNG-II, J., GALLAGHER-III, J.S., NORMAN, M.L., BALLESTER, G.E., BURROWS, C.J., CASERTANO, S., CLARKE, J.T., CRISP D., GRIFFITHS, R.E., HOESSEL, J.G., HOLTZMAN, J.A., KRIST, J.E., MOULD, J.R., SANKRIT, R., STAPELFELDT, K.R., TRAUGER, J.T., WATSON, A.M. & WESTPHAL, J.A. (1996) WFPC2 Studies of the Crab Nebula. III. Magnetic Rayleigh-Taylor Instabilities and the Origin of the Filaments. *Astrophysical Journal* **456**, p.225

KIRK, A., WILSON, H.R., AKERS, R., CONWAY, N.J., COUNSELL, G.F., COWLEY, S.C., DOWLING, J., DUDSON, B., FIELD, A., LOTT, F., LLOYD, B., MARTIN, R., MEYER, H., PRICE, M., TAYLOR, D., WALSH, M. & the MAST team, (2005) Structure of ELMs in MAST and the implications for energy deposition. *Plasma Phys. Control. Fusion* **47**, 315

LEHNERT, B. (1971) Rotating Plasmas. *Nucl. Fusion* **11** 485

LOUEIRO, N.F. & UZDENSKY, D.A. (2016) Magnetic reconnection: from the Sweet-Parker model to stochastic plasmoid chains. *Plasma Phys. Control. Fusion* **58**, 014021

MICOZZI, P., ALLADIO, F., MANCUSO, A. & ROGIER, F. (2010) Ideal MHD stability limits of the PROTO-SPHERA configuration. *Nucl. Fusion* **50**, 1-10

NAGATA, M., KANKI, T., MASUDA, T., NAITO, S., TATSUMI, H. & UYAMA, T. (1993) Relaxation oscillations and toroidal-current regeneration in a helicity-driven spheromak. *Phys. Rev. Lett.* **71**, 4342

PARKER, C.A., HOBBS, L.W., RUSSEL, K.C. & CLINARD JR., F.W. (1985) Damage Structures in Fast Neutron Irradiated Magnesium Aluminate and Electron Irradiated Aluminum Oxynitride Spinels. *Journal of Nuclear Materials* **133**&**134** 741-744

PARKER, E.N. (1990) Intrinsic magnetic discontinuities and solar X-ray emission. *Geophys. Res. Lett.* **17**, 2055

PAULOS, R.D., TRONE, M. & KUCZAJ, S.A. (2010) Play in Wild and Captive Cetaceans. *International Journal of Comparative Psychology* **23**, 701-722

ROGIER, F., BRACCO, G., MANCUSO, A., MICOZZI, P. & ALLADIO, F. (2003) Simply Connected High-Beta Magnetic Configurations. *11th International Congress on Plasma Physics: ICPP 2002, AIP Conference Proceedings* **669**, 557

SHAFRANOV, V.D. (1966) Plasma Equilibrium in a Magnetic Field. *Reviews of Plasma Physics, ed M A Leontovich (New York: Consultants Bureau),* Vol **2***,* p. 103

SOUTHWOOD, D.J., FARRIJGIA, C.J. & SAUNDERS, M.A. (1988) What Are Flux Transfer Events?. *Planet. Space Sci.* **36**, 505-508

STENZEL, R.L. & GEKELMAN, W. (1981) Magnetic Field Line Reconnection Experiments 1. Field Topologies. *Journal of Geophysical Research* **86**, 649-658

STENZEL, R.L., GEKELMAN, W. & WILD, N. (1982) Magnetic Field Line Reconnection Experiments 4. Resistivity, Heating, and Energy Flow. *Journal of Geophysical Research* **87**, 111-117

SPRUIT, H.C. (2013) Essential magnetohydrodynamics for astrophysics. (http://arxiv.org/abs/1301.5572)

TAVANI, M., BULGARELLI, A., VITTORINI, V., PELLIZZONI, A., STRIANI, E., CARAVEO, P., WEISSKOPF, M.C., TENNAN, A., PUCELLA, G., TROIS, A., COSTA, E., EVANGELISTA, Y., PITTORI, C., VERRECCHIA, F., DEL MONTE, E., CAMPANA, R., PILIA, M., DE LUCA, A., DONNARUMMA, I., HORNS, D., FERRIGNO, C., HEINKE, C.O., TRIFOGLIO, M., GIANOTTI, F, VERCELLONE, S., ARGAN, A., BARBIELLINI G., CATTANEO, P.W., CHEN, A.W., CONTESSI, T., D'AMMANDO, F., DEPARIS, G., DI COCCO, G., DI PERSIO, G., FEROCI, M., FERRARI, A., GALLI, M., GIULIANI, A., GIUSTI, M., LABANTI, C., LAPSHOV, I., LAZZAROTTO, F., LIPARI, P., LONGO, F., FUSCHINO, F., MARISALDI, M., MEREGHETTI, S., MORELLI, E., MORETTI, E., MORSELLI, A., PACCIANI, L., PEROTTI, F., PIANO, G., PICOZZA, P., PREST, M., RAPISARDA, M., RAPPOLDI, A., RUBINI, A., SABATINI, S., SOFFITTA, P., VALLAZZA, E., ZAMBRA, A., ZANELLO, D., LUCARELLI, F., SANTOLAMAZZA, P., GIOMMI, P., SALOTTI, L. & BIGNAMI, G.F. (2011) Discovery of Powerful Gamma-Ray Flares from the Crab Nebula. *Science* Vol. **331**, Issue 6018, pp. 736-73

TAYLOR, J.B. & TURNER, M.F. Plasma current drive by helicity injection in relaxed states. (1989) *Nucl. Fusion* **29**, 219-229

TUSZEWSKI, M. (1988) Field Reversed Configurations. *Nucl. Fusion* **28**, 2033

VELASCO FUENTES, O. (2014) Early observations and experiments on ring vortices. *European Journal of Mechanics B/Fluids* **43**, 166–171

VELIKHOV, E.P. (1959) Stability of an Ideally Conducting Liquid Flowing between Cylinders Rotating in a Magnetic Field. *Sov. Phys. JETP* **36,** 995

WESSON, J. (2011) Tokamaks**. 4th ed**., Oxford University Press, Oxford

ZWEIBEL, E.G. & YAMADA, (2009) Magnetic Reconnection in Astrophysical and Laboratory Plasmas. *Annu. Rev. Astron. Astrophys.* **47**, 291–332

ZWEIBEL, E.G. & YAMADA, M. (2016) M. Perspectives on magnetic reconnection. *Proc. R. Soc.* **A 472**, 20160479